# Bond behaviour of concrete-filled steel tubes at the Arctic low temperatures

Jia-Bao Yan, Wenjun Xie, Lingxin Zhang, Xu-Chuan Lin

Version of Record: https://www.sciencedirect.com/science/article/pii/S0950061819306415
Manuscript_b77c780c97bc92dbbb39c9aef792116d

# Bond behaviour of concrete-filled steel tubes at the Arctic low temperatures

Jia-Bao Yan[a], Wenjun Xie[a], Lingxin Zhang[b,*], Xu-Chuan Lin [b]

[a]*School of Civil Engineering / Key Laboratory of Coast Civil Structure Safety of Ministry of Education, Tianjin University, Tianjin 300350, China*
[b]*Key Laboratory of Earthquake Engineering and Engineering Vibration, Institute of Engineering Mechanics, CEA, Harbin 150080, China*

**Abstract:** This paper investigated bond behaviour of concrete-filled steel tube (CFST) columns at the Arctic low temperatures. A testing program with ten square and ten circular CFSTs were tested under different low temperatures ranging from 30ºC to -80ºC. The influences of different low temperature levels, diameter to thickness ratio (*D/t*), grades of concrete, length to diameter ratio (*L/D*), and cross-section type were checked through these 20 tests. The test results showed that the Arctic low temperatures significantly improved the bond behaviour of the CFST columns; lower grade concrete exhibited larger ultimate bond strength ($\tau_u$); increasing *D/t* ratio reduces the ultimate bond strength; *L/D* ratio has marginal influences on $\tau_u$ values; and circular CFST columns exhibited higher ultimate bond strength than those of square ones. Different from the CFST column at ambient temperature, the frozen-ice bond for the CFST columns at low temperature improves its ultimate bond strength. A prediction equation was proposed for ultimate bond strength of CFST columns at low temperatures. The validations against the reported 20 tests show that the proposed equation offered conservative predictions but more accurate predictions than the design codes, e.g., Eurocode 4 and ANSI/AISC.

**Keywords:** Bond behaviour; Push-out test; CFST column; Low temperature; Ultimate bond strength; Arctic structure; Composite structures.
***Corresponding author**: Lingxin Zhang, E-mail address: lingxin_zh@126.com

## Nomenclature

$D$ = External Diameter or width of the circular (or square) CFST column

$L$ = Length of the CFST column.

$P$ =Applied load in push-out tests

$T$ =Temperature level, in ºC555

$f_{cu}$ =Compressive strength of concrete cube

$f_{cu,T}$ =Compressive strength of concrete at low temperatures

$f_{cu,a}$ = Compressive strength of concrete at ambient temperatures

$f_y$ = Yield strength

w/c=Water-to-cement ratio

$t$ = Thickness of the wall in steel tube

$\tau$ = Bond stress

$\tau_u$ = Ultimate bond strength

$\tau_{u,t}$ =Experimental ultimate bond strength

$\tau_{u,p}$ =Predicted ultimate bond strength

## Abbreviations

CAB, chemical adhesion bond; CFST, concrete filled steel tube; CCFST, circular concrete filled steel tube; SCFST, square concrete filled steel tube; COV, coefficient of variation; FIB, frozen-ice bond; LNG, liquid nitrogen gas; LVDT, linear varying displacement transducers; MI-LB, micro-locking bond; MA-LB, macro-locking bond.

## 1 Introduction

Concrete filled steel tube (CFST) columns, consisting of an external steel tube and a concrete core, have been developed and put into use in engineering constructions in recent several decades. This type of composite structure utilizes the concrete compression and steel tension that exhibits extensive advantages of high strength and ductility, easy construction, and excellent seismic performance. In addition, the external steel tubes saves formwork, site construction costs, labour forces that resulted in the improved construction efficiency. CFST columns have been extensively used as the columns or other structural elements in high-rise buildings and bridges. More recently, more and more steel-concrete composite infrastructures has been built in the cold regions even in the Arctic region, e.g., composite bridges in northern and Tibet of China. Fig. 1 shows the typical CFST column bridge piers in the cold regions.

In the cold and Arctic region, the engineering infrastructures were exposed to the environment with low temperatures. The recorded lowest temperature in Tibet, China is about -60°C [1]. In the Arctic region, this lowest recorded temperature could be even lower to -70°C [2]. Such low temperatures bring impacts on the mechanical properties of the constructional materials [3-6] in CFST columns as well as the bond strength at steel-concrete interface in composite structures [7]. Thus, it is of importance to investigate these mechanical properties and bond strength of CFST columns at low or even ultra-low temperatures relevant to the cold region and the Arctic environment.

Bond strength acts essentially on stress transferring between the concrete core and

steel tube in the CFST column. It also plays important roles on preventing steel tube from local buckling, providing permanent formwork, offering steel-concrete bond strength that make sure the two different component work compositely to resist the external different loadings of tension, torsion, shear, and bending moment. Thus, this bond strength is important to the structural behaviours of CFST columns. Extensive previous studies have been carried out to investigate the bond strength of CFST columns at ambient or high temperatures. Virdi and Dowling [8] performed pioneer research on the bond strength at steel tube-concrete interface through push-out tests on CFST columns. The key parameters including mechanical properties and curing conditions of the concrete as well as geometry were selected in the reported testing program. Continued works was contributed by Morishita et al. [9] and Tomii et al. [10] in the 1980s. Shakir-Khalil [11] also experimental push-out strength at ambient temperatures. Roeder et al. [12] studied the bond behaviours of concrete filled tubes with larger diameter than those used in Japan. Hunaiti [13, 14] studied the steel tube-concrete bond strength in battened columns and the influence of aging of concrete on this bond strength. Petrus et al. [15] studied the improvement of tab stiffeners on the bond strength in CFST columns. Continuous improvements on this bonding strength were achieved through using bolts [16-17], tab stiffeners [15], and self-taping screws [18], and headed studs [19]. Aly et al. [20] and Qu et al. [21] also contributed to this topic of bond strength at ambient temperatures. More recently, the steel-concrete bond strength post fire have been experimentally studied [22-23]. Song et al. [24] experimentally studied the steel-concrete bond strength of CFST at elevated

temperatures. All these studies focused on the scenario of the CFST columns exposed to the fire hazard. Thus, it can be found that all these past studies concentrated on the bond strength at steel tube-concrete interacting surface at ambient or high temperature. The studies on the concrete-steel tube bond strength at low temperatures relevant to the cold and Arctic regions are still quite limited. This bond behaviour so far have not been fully understood. From this point of view, it is necessary to carry out push-out tests on CFST columns at the Arctic low temperatures to obtain necessary information on the concrete-steel tube bond strength of at the low temperatures. All these would offer useful information on designing CFST columns in the cold and Arctic regions, and promote the engineering applications of the CFST columns in cold regions.

This paper firstly studied the steel tube-concrete bond strength b at different Arctic low temperatures through 20 push-out tests. The influences of different parameters on the bond strength at low temperatures were studied, i.e., low temperatures, diameter to thickness ratio, different grades of concrete core, and length over diameter ratio. Based on the reported test results, these influences on bond strength of the CFST were analysed and discussed. Including the experimental studies, the prediction equation was also developed to determine the ultimate bond strength of CFST columns at low temperatures.

## 2 Testing programme

### 2.1 Details of specimens

Twenty stub CFST columns were prepared for the push-out tests. The parameters

selected in this testing programme included the shape of the cross section for CFST column (i.e., circular and square cross section), low temperature level $T$, strength of concrete core $f_c$, diameter to thickness ratio ($D/t$) through fixing the diameter but using steel tube in different thickness $t$, and interface length to diameter (or width) ratio $L/D$ .

Two batches of specimens consisting of ten specimens in each batch were designed with circular and square cross section, respectively. The same parameters were studied in each batch.

To study the influence of low temperatures, specimens C1~4 and S1~4 were tested at temperatures of 30°C, -30°C, -60°C and -80°C, respectively. Since different grade concrete tends to have different w/c ratio that would affect the bonding strength of CFST, specimens C5 and S5 were designed with C30 whilst C6 and S6 were designed with C60 normal weight concrete, which were compared to C1 and S1 designed with C45 concrete. Mix proportions for C30, C45 and C60 concrete are given in Table 1. In order to study the effect of $D/t$, specimens C7 and S7 were fabricated with 3mm-thick steel tube whilst C8 and S8 were made of 6 mm-thick steel tube, which are different from 4 mm-thick steel tube used for the rest specimens. In order to study $L/D$ ratio on the bonding strength of the CFST column, specimens C1, C9, and C10 were designed with $L/D$ ratios of 2.71, 1.58, and 4.21, respectively; specimens S1, S9, and S10 were designed with $L/D$ ratios of 3.0, 1.75, and 4.25, respectively.

Each specimen, consisting of a steel tube and a concrete core, measures 133 mm (or

120 mm) in diameter (or width) and 400 mm in length, respectively except those prepared for the length to diameter (or width) ratio. All the specimens were reserved a gap of 10 mm at the top to locate the steel block for the loading purpose. For each specimen, a gap of 30 mm was reserved between the bottom end of the steel tube and lower free surface of concrete core to make sure the slip capacity of inside concrete core. (see Fig. 2).

The yield strength and elastic Young's modulus at ambient temperatures for the steel tube in all the specimens are 320 MPa and 200 GPa, respectively. Table 2 list both geometric and material details for 20 specimens.

Figure 3 shows the preparation of CFST columns before and after casting of concrete. All the specimens were tested at 28 days after casting of the concrete.

### 2.2 Setup of push-out tests

Figure 2 shows the setup of push-out tests on CFST columns at low temperatures. Before testing, the specimen was firstly moved into a cold storage to make sure achieving target testing temperature, and it was maintained at this temperature level for 48 hours as specified in Chinese code GB51081-2015 [25]. After that, the CFST column was installed into the 300-ton testing machine with a cooling chamber surrounding the specimen. The low temperature environment was thus simulated by this cooling chamber. The cooling chamber was made of insulation materials that minimizes the heat transfer between the specimens and room environment. Moreover, liquid nitrogen gas (LNG) was also injected into the cooling chamber to maintain the

target testing temperature levels (as shown in Fig. 2(b)). During this testing process, a PT 100 thermocouple embedded in the CFST column with another four thermocouples installed at four corner of the cooling chambers were used to monitor the temperature in the specimen as well as in the chamber. All these readings were used to control the injection-flow velocity of the LNG that could maintain the testing temperature. After achieving the low temperature, displacement loading was applied to the loading end plate through the testing machine in a slow rate of 0.1 mm/min.

Each CFST column was designed with a 30 mm air gap between the bottom end and inside bottom surface of the concrete core. The relative slip at this free end was measured by a steel bar that was embedded in the concrete core during the casting and extended out from the specimen. A horizontal steel angle was connected to this embedded steel bar and extended out from cooling chamber that facilitates the measurements of the slip at the free end (see Fig. 2). Two linear varying displacement transducers (LVDTs) were attached to the extending steel angle to measure the slip at free end (see Fig. 2). Meanwhile, four LVDTs were installed to measure the slip occurred to the loading end. A load cell as shown in Fig. 2(b) was installed next to the loading plate to record the reaction forces during the loading progress. Strain gauges were attached to the steel tubes to measure the strains in both horizontal and vertical directions at three different locations as shown in Fig. 2(b).

The readings of slips by LVDT, strains by strain gauges, and reactions forces recorded by the load cell were recorded by a connected data logger.

## 3 Test results

There are no obvious changes in the concrete core and steel tube except the occurrence of slip between the steel tube and concrete. No local buckling or concrete crushing were observed during the testing progress.

### 3.1 Bond stress versus slip behaviours

To estimate the bond capacity at the steel-concrete interface, the average bond stress was adopted as the following;

$$\tau = \begin{cases} P/[\pi(D-2t)L] & \text{for circular CFST} \\ P/[4(D-2t)L] & \text{for square CFST} \end{cases} \quad (1)$$

where, $P$ denotes applied load; $D$ denotes external diameter or width of the circular (or square) CFST column; $L$ denotes the Length of the CFST column.

Fig. 4 and 5 shows the $\tau$ versus slip $S$ at the loading end curves for circular and square CFST columns, respectively. These two figures show that these $\tau$-$S$ curves can be categorized into four types as concluded in Fig. 6. In the first three types of $\tau$-$S$ curve, the bond stress increases linearly with the increasing slip until achieving about 80%~90% ultimate value. After the peak resistance, the bond stress decreases by about 5%~20% as the slip increases. After that, the bond stress versus slip curves exhibit three different behaviours in type I~III $\tau$-$S$ curves. Type I $\tau$-$S$ curve exhibits fast increase in the bond stress as the slip increases; type II curve exhibits relative lower increasing magnitude of the bond stress as the slip increases, and the difference between the first and second peak bond stress is quite limited; type III curve exhibits

decrease of the bond stress in a slow rate or even flat plateau of the $\tau$-$S$ curves. The only difference among these three types of $\tau$-$S$ curve exist only in the post-peak recession stage. $\tau$-$S$ curves of specimens C2, C3, and C6 are belonged to type I; $\tau$-$S$ curves of specimens C1, C4, C7, C8, C9, S1-4, and S6-10 are belonged to the second type of curve; curve of C10 is belonged to type III, and curves of S5 and C5 are belonged to type IV.

In the first three types of bond stress versus slip curves, the first peak resistance was contributed by the chemical adhesion, micro-locking, and frozen-ice adhesion. The chemical adhesion is determined by the capillary action that was produced by the cement hydration. This chemical adhesion is affected by many factors, e.g., w/c ratio. The micro-locking is mainly influenced by the interfacial roughness of the steel tube. Different from the CFST column at ambient temperatures, at low temperatures the water in the capillary and open pores at the steel-concrete interface tends to be frozen, which increases the bond stress of the push-out tests on CFST column. After point B, during the recession stage, the chemical adhesion bond and frozen-ice bond tends to fail, and macro-locking tends to govern the bond stress versus slip behaviours. The macro-bonding is mainly produced by the non-uniformity in the straightness or in the diameter of steel tube that were mainly due to the manufacture tolerance. If this non-uniformity in the straightness or diameter of steel tube is large, the increasing magnitude of bond stress after the first peak tends be larger than that of the rest two types of curves that exhibit much larger slope in the $\tau$-$S$ curve after achieving first peak value, i.e., curve CF in Fig. 6(a). In case of the non-uniformity in the

straightness or diameter of the steel tube is small, the bond stress would decrease gradually with the increasing slip, i.e., curve CD in the type III $\tau$-$S$ curve as shown in Fig. 6(a). If the non-uniformity in the straightness or diameter is intermediate, the bond stress after the first peak value tends to remain constant or slightly increases/decreases, i.e., type II curve in Fig. 6(a).

Type IV $\tau$-$S$ curve exhibits different manner from type I~III curves. In type IV $\tau$-$S$ curve, the bond stress firstly increases almost linearly with the increasing slip until achieving the peak value, and then exhibits a sharp drop to its 50% ultimate value. The $\tau$-$S$ curves of specimens with C30 grade concrete (i.e., specimens C5 and S5) were belonged to this category. Moreover, the ultimate bond stresses of C5 and S5 are much larger than the rest specimens. This may be due to that the C30 normal weight concrete in the CFST column was designed with much larger w/c ratio. This leads to much larger frozen-ice bond stress at the concrete-tube interface. The frozen-ice bond stress is more brittle compared with the micro-locking bond stress and chemical adhesion, and this may explain the large magnitude of decrease of the bond stress after the first peak resistance. After the first peak, the chemical bond stress, micro-locking, and frozen-ice bond stress lost their functions, and only macro-locking takes effect that results in much flat and stable bond stress versus slip behaviours.

### 3.2 Strain distribution on the external surface of steel tube along height of CFST column

Figure 7 shows the distribution of strain along the height of steel tube at different loading levels for representative specimens at different low temperatures. It shows

that at initial different loading levels the strain increases almost linearly with the distance from the loading end, and the strain near the free end is much larger than that at the loading end. Most of the strain versus distance from the loaded end curves are in triangular shape that implies the even distribution of the bond stress along the height of CFST column. In addition, the strains at different locations increase with the applied load that implies the chemical adhesion, ice-frozen adhesion and micro-bonding takes effect. After the peak load, non-uniform distribution of the strains along the height of the column is observed, which implies the failure of the chemical and micro-bonding, and the macro-bonding takes effect. One interesting observation is that all the strain versus distance curves firstly increases with the distance from the loaded end but exhibit certain degree of decrease at the free end, which may be produced by the "pinching effect" at the free end as pointed by Tao et al. [22] .

### 3.3 Discussions on influences of different parameters

#### *3.3.1 Influence of low temperatures*

Fig. 8(a) depicts the effect of low temperatures on ultimate bond strength $\tau_u$. It shows that the low temperature $T$ exhibits significant improvements on the ultimate bond strengths for the circular CFST column (CCFST) and square CFST column (SCFST). It can be also found that both the ultimate bond strengths for CCFST and SCFST increase almost linearly as the temperature decreases. As the $T$ value drops down from 30°C to -30°C, -60°C, and -80°C, the $\tau_u$ value of the circular CFST column was

significantly increased by 190%, 248%, and 287%, respectively whilst the $\tau_u$ value of the square CFST column was increased by 55%, 167%, 215%, respectively. Fig. 8(a) also shows that the increments of the ultimate bond strength for the CCFST columns are much larger than those SCFST values at the same low temperature level, which implies that the effect of the low temperatures on the ultimate bond strength of CCFST columns is more significant than on the square ones.

These increments in ultimate bond strength produced by the low temperature were due to the following reasons;

(1) At low temperatures, the coefficients of thermal expansion, $\alpha_s$, of steel tends to be larger than that of concrete, $\alpha_c$, e.g., the $\alpha_s$ for steel at low temperatures of 30~ -80°C are about 11.8~9.4 x$10^{-6}$/°C [26], and the $\alpha_c$ values for normal weight concrete at low temperatures of 30~ -80°C are about 6.85~6.00 x$10^{-6}$/°C, respectively [27, 28]. This means the steel tends to contract faster than the concrete at low temperatures. Thus, the confining stress between the steel tube and concrete tends to increase at low temperatures, which results in increased friction force as well as bond strength. Moreover, previous studies [29, 30] also observed that the concrete tends to expansion at low temperatures of -20 °C to -70 °C, which further increases the confining stress and thus the bond strength at low temperatures.

(2) Low temperature improves the compactness of micro-structure of the normal weight concrete that increases the roughness of the steel-concrete interface. Under low temperatures, the water in pores and micro-cracks changes into ice and increases the micro-lock bond strength of the CFST column. However, previous studies also

shows that freezing into ice temperature of the water changes gradually in the capillary pores that were mainly influenced by the size of the pores and salt concentration in them [31]. Fig. 9 depicts the freezing temperature versus pore radius relationship [31]. It can be found that the freezing temperature of water in different size of pore varies from 0 to -80℃, which explains the continuous increasing of the ultimate bond strength of CFST as $T$ drops down from 30°C to -80°C.

(3) The frozen water at the steel tube-concrete core interface produces additional bond stress that act similarly to the chemical adhesion bond. Since the internal concrete is sealed by the external tube, this prevents evaporation of the water in the surface of the concrete core. After exposure of the CFST column to low temperatures, the water at steel-concrete interface tends to be frozen and resulted in additional bond stress, which exhibits different mechanism from that at ambient temperatures.

(4) At low temperatures, due to different thermal expansion behaviours for steel and concrete, the external steel tube tends to contract whilst the frozen ice in the capillary pore and gel pore of the concrete tends to expand that minimize the contraction of the NWC. Thus, the contracting steel tube would improves the ultimate bond strength of the specimen.

Thus, this significant influence of low temperatures on the bond behaviour of CFST column needs to be well considered.

### *3.3.2 Influence of different grade of concrete*

Fig. 8(b) depicts the effect of different grade of concrete on the ultimate bond strength of CFST column. This figure shows an interesting finding that under low temperature of -60ºC the CFST column with lower grade normal weight concrete (NWC) exhibits higher ultimate bond strength. As shown in this figure, reducing the grade of NWC from C60 to C45 and C30 the ultimate bond strength of the CCFST is increased from 1.31 MPa to 2.15MPa and 3.51 MPa, respectively whilst the ultimate bond strength of SCFST is increased from 1.29 MPa to 1.55 MPa and 2.22 MPa, respectively. At low temperature of -60°C, the compressive strength of the C30, C45, and C60 are 47.2 MPa, 53.5MPa, and 65.5MPa, respectively. However, the lower strength concrete leads to higher ultimate bond strength. This can be explained by that the lower strength was designed with higher water-to-cement (w/c) ratio, which is more porous and contains more water. Once exposed to low temperature, the water at the steel tube-concrete interface tends to be frozen that results in new bond stress, which results in higher ultimate bond strength. However, this bond strength produced by the frozen ice cannot be quantified since it relates to the water content, w/c ratio, and temperature levels. More studies are still required to investigate this ice-frozen bond strength.

### *3.3.3 Influence of diameter-to-thickness (D/t) ratio*

Fig. 8(c) depicts the influence of *D/t* ratio on the ultimate bond strength of both CCFST and SCFST at -60°C. It shows that at -60°C the ultimate bond strength for both square and CCFST columns is in negative linear relationship with the increasing

*D/t* ratio. As the *D/t* ratio increases from 23.1 to 29.6 and 44.3, the ultimate bond strengths are both reduced by 20% for CCFST. Meanwhile, for square CFST column, as the *D/t* ratio increases from 24 to 43.6, the ultimate bond strength is reduced by 30%. This can be explained by that increasing the thickness of steel tube results in higher confinement to internal concrete. All these resulted in improved ultimate bond strength. Similar findings have been reported in Refs. [12, 22, 32]. Thus, this *D/t* ratio on $\tau_u$ of the CFST columns at low temperatures need to be well considered.

### *3.3.4 Influence of length to diameter (L/D) ratio*

Fig. 8(d) depicts the influence of *L/D* ratio on $\tau_u$ of the CFST column at low temperature of -60°C. It shows that the *L/D* ratio exhibits totally opposite effects on $\tau_u$ for CCFST and SCFST. The increasing *L/D* ratio has slightly positive influence on $\tau_u$ of the CCFST. As the *L/D* ratio increases from 1.6 to 2.7 and 4.2, the ultimate bond strength of the circular CFST column is slightly increased by 1% and 8%, respectively. However, as the *L/D* ratio increases from 1.75 to 3.00 and 4.25, the ultimate bond strength of the square CFST column is decreased by 23% and 13%, respectively. Moreover, the correlation coefficient of $\tau_u$ with *L/D* ratio is only 0.29 that implies weak correlation between the ultimate bond strength and *L/D* ratio. Thus, the effects of *L/D* ratio on $\tau_u$ of the CFST column at low temperature -60°C are controversial for circular and square CFST columns, and this effect may be neglected based on these limited test data.

### *3.3.5 Influence of cross-section type*

Since the first batch of circular CFST columns C1~10 were designed with the same geometry and materials and tested at the same condition with SCFST columns S1~10, Fig. 10 compares their ultimate bond strengths at different temperatures. It shows that the ultimate bond strength of CCFST columns are larger than those of SCFST at low temperatures. For the prepared ten specimens, the ultimate bond strength of circular CFST is averagely 46% larger than that of SCFST. This difference tends to be larger for the CFST designed with thinner steel tube and low grade NWC, e.g., the ultimate bond strength of specimen C7 with 2.75 mm thick steel tube is 2.14 times of that for specimen S7. This is because the circular shape of steel tube transfers the steel-concrete interfacial bond stress more effectively than the square steel tube. At the working state, the steel tube tends to suffer outward pressure and vertical compression. Outward buckling more likely occurred to the flat side plate in square steel tube than circular steel tube, which results in separation at the steel tube-concrete interface and reduced the ultimate bond strength. The bond stress in square CFST columns were thus mainly taken by the corner regions in square CFST columns. This phenomena tends to be more serious for the square steel tube with lower thickness and suffering larger bond stress. This may explain the large circular-to-square ratios of ultimate bond strength in specimens C3-4, C7, and C8.

## 3.4 Mechanism of bond stress for CFST column at low temperatures

### *3.4.1 Components of bond stress for CFST column at low temperatures*

There are four components of the bond stress in CFST column at low temperatures, i.e., chemical adhesion bond, micro-locking bond, macro-bonding, and frozen-ice adhesion bond.

**(1) Chemical adhesion bond**

The hydration gel of concrete produces chemical adhesion bond stress at the steel-concrete interface (see Fig. 11(a)). According to previous studies, this chemical adhesion bond tends to fail at low slip level at the interface [34]. This chemical adhesion bonds is usually influenced by the cement and water-to-cement ratio in the mix proportions.

**(2) Micro-locking bond**

The micro-locking bond stress is shown in Fig. 11(b). This bond stress was mainly produced by the reaction crushing force acting on the mechanical keys due to the roughness of internal surface of steel tube (see Fig. 11(b)). Since the roughness of the internal surface of steel tube was at about 0.01 mm level, it was also called micro-tolerance. Previous studies showed that the micro-locking bond stress was mainly determined by the roughness of the steel tube's internal surface and only took effect before the free sliding of internal concrete core, which implies this bond stress contributes to the ultimate bond strength [8].

**(3) Macro-locking bond**

The manufacture tolerance in the diameter and thickness along the height of the steel tube resulted in the sliding friction resistance as shown in Fig. 11(c), i.e., macro-locking bond. This bond usually determines the post-peak strength behaviour in the τ-*S* curves. As shown in Fig. 11(c), in case of the internal diameter of steel tube shrinks at the mid-height, the sliding-down concrete will be resisted by the thrust forces provided by the internal wall of steel tube due to wedge effect. The manufacture tolerance of inner diameter of steel tube determines this macro-locking bond strength.

**(4) Frozen-ice bond**

Fig. 11(d) shows the mechanism of the frozen-ice bond in the CFST column at low temperatures. The steel tube in CFST column effectively prevents evaporation of water into air. Thus, at low temperatures, the water at the interface tends to be frozen that resulted in additional adhesion stress and improved roughness of the internal surface (i.e., macro-locking bong strength). As shown in Fig. 4(a) and 5(a), the low temperature significantly improved the bond behaviour of the CFST column that needs well consideration.

### *3.4.2 Mechanism of bond stress for CFST column at low temperatures*

Fig. 12 illustrates the mechanisms of the development of bond stress-slip behaviours. Fig. 13 depicts the bond stress versus slip curves at loaded and free ends of CFST columns. Fig. 12(a) and 13 shows that at the early stage of push-out tests there is no slip occurred at the steel-concrete interface; the bond stress mainly consists of

chemical adhesion bond (CAB) and frozen-ice bond (FIB). This can be reflected on the load versus slip at free end curves of the specimens. After that at point “b” in Fig. 12(b), as the applied load increases, slip occurs in the local regions at both ends of the CFST columns due to failure of the CAB. Meanwhile, micro-locking bond (MI-LB) starts to work. As the applied load further increases, the slips at both ends continue increasing and propagate from the ends to the middle region where no slip occurred. Meanwhile, the CAB and FIB only exists at the middle region of the specimens as shown in Fig. 12(c). Finally, at point “d” as shown in Fig. 12(d), the CFST achieves its ultimate bond strength that equals to the sum of CAB, FIB, and MI-LB. Moreover, at point “d”, slip fully occurred to the concrete-steel tube interface. After the peak loads, the concrete core slide freely along the height direction; meanwhile, CAB and FIB failed and the applied load was only taken by the interfacial friction as shown in Fig. 12(e). After that, macro-locking bond (MA-LB) took place that determines the bond stress as shown in Fig. 12(f).

## 4 Comparisons of predictions by design codes with reported test results

The literature review shows that it is still difficult to provide an accurate theoretical model on ultimate bond strength of CFST columns [19]. In Eurocode 4 [35], the ultimate bond strength of SCFST and CCFST at ambient temperature are specified as 0.4 MPa and 0.55 MPa, respectively. In ANSI/AISC360-10 [36], this ultimate bond strength is specified as 0.4 MPa. Cai [37] has proposed a following formula to predict the ultimate bond strength of the CFST column at ambient temperature;

$$\tau_u = 0.1 f_{cu}^{0.4} \quad (2)$$

where, $f_{cu}$ denotes cubic compressive strength of concrete.

Since the low temperature exhibited significant effect on $\tau_u$ of CFST columns, with the reported test results, following modifications on equations in Eurocode 4 [35] were used to incorporate this influence;

$$\tau_u = \begin{cases} (1.88\text{-}0.026T)\times 0.55 & \text{for circular CFST} \\ (1.41\text{-}0.020T)\times 0.40 & \text{for square CFST} \end{cases} \quad (3)$$

where, $T$ denotes temperature, in ºC.

Fig. 14 compares the reported 20 test results with those predictions by proposed Eqn. (3), Eurocode 4 [35], and ANSI/AISC360-10 [36]. It can be found that the design codes Eurocode 4 [35] and ANSI/AISC360-10 provide much more conservative predictions on the $\tau_u$ values of CFST columns at both ambient and low temperatures. Even though the proposed Eqn. (3) provides more accurate predictions on $\tau_u$ compared with code equations, it is still very conservative. For the 20 tests, the mean test-to-prediction ratio is 1.36 with a Cov of 0.27. However, this prediction equation was only validated by 20 tests at low temperatures. Moreover, the influence of the *D/t* ratio, w/c ratio, and bond strength of the ice have not considered in the prediction equation due to insufficient test data. More test results on bond strength at low temperatures of CFST columns are still required for the development of more accurate prediction equations.

## 5 Conclusions

This paper makes efforts to study the bond behaviour of CFST columns at low temperatures. 20 push-out tests were performed on both square and circular columns at low temperatures. Different parameters were studied in the testing programme that included low temperature level, grades of concrete, *D/t* ratio, and *L/D* ratio. Including the reported test results, available prediction equations in design codes and literature were used for the prediction on the ultimate bond strength of the CFST columns at low temperatures. From these studies, the conclusions can be drawn as the following;

(1) Bond behaviours of CFST columns were improved at the Arctic low temperature, and the circular CFST columns exhibited larger ultimate bond strengths than the square CFST columns. Decreasing the temperature from 30°C to -30°C, -60°C, and -80°C increases the ultimate bond strength of CCFST columns by 190%, 248%, and 287%, respectively. Meanwhile, these increments of ultimate bond strength for the square CFST column are 55%, 167%, and 215%, respectively. The improved bond strength of the CFST column was due to increased compressive strength of concrete and frozen of the water at steel tube-concrete interface.

(2) At low temperatures, using lower strength NWC in the CFST column received higher ultimate bond strength. As the grade of NWC decreases from C60 to C45 and C30 the ultimate bond strength of CCFST was increased by 64% and 168%, respectively, and the increments of ultimate bond strength for SCFST are 20% and 72%, respectively. These improved ultimate bond strengths were due to the

containment of more water at steel tube-concrete interface, which was converted into ice at low temperatures.

(3) Increasing the *D/t* ratio at low temperature of -60ºC from about 23 to 44, ultimate bond strengths of CCFST and SCFST column were reduced by 20% and 30%, respectively due to the reduced confinement of the steel tube on the concrete core.

(4) Increasing the *L/D* ratio of CFST columns exhibits opposite and limited influences on the ultimate bond strength on CCFST and SCFST columns at -60ºC. As the *L/D* ratio increases from 1.6 to 2.7 and 4.2, the ultimate bond strength of CCFST column is slightly increased by 1% and 8%, respectively. However, as the *L/D* ratio increases from 1.75 to 3.00 and 4.25, the ultimate bond strength of the square CFST column is decreased by 23% and 13%, respectively.

(5) The ultimate bond strength of CCFST columns are larger than SCFST columns at low temperatures. The ultimate bond strength of CCFST is averagely 46% larger than that of SCFST columns due to the more effective transfer on steel-concrete interfacial bond stress.

(6) There are four components in the steel-concrete bond strength of CFST columns at low temperatures, i.e., chemical adhesion bond, micro-locking bond, macro-locking bond, and frozen-ice bond. The frozen-ice bond increases both ultimate bond strength and post first peak bond strength.

(7) Prediction equation was proposed for ultimate bond strength of CFST columns at low temperatures. Compared with the prediction equations in EC4 and ANSI/AISC, the proposed equations improves the accuracy of the predictions on

ultimate bond strength of CFST columns, but still offer conservative predictions compared with the test results.

(8) The proposed equation was validated by limited test data, further more tests are still required for the validation purpose as well as investigations on influences of different parameters.

## ACKNOWLEDGMENT

The authors would like to acknowledge the research grant 51608358 and 51678542 received from National Natural Science Foundation of China, and Peiyang Scholar Foundation (grant no. 2019XRX-0026) under Reserved Academic Program from Tianjin University for the works reported herein. The authors gratefully express their gratitude for the financial supports.

## Conflicts of interest statement

The authors declare that they have no conflicts of interests.

## References

[1] Qiao Y, Wang HF, Cai LC, Zhang W, Yang BH. Influence of low temperature on dynamic behavior of concrete. Construction and Building Materials 2016; 115: 214-220.
[2] Gautier DL, Bird KJ, Charpentier RR, et al., Assessment of undiscovered oil and gas in the arctic. Science 2009; 324 (5931): 1175–1179.
[3] Xie J, Zhu GR, Yan JB. Mechanical properties of headed studs at low temperatures in the Arctic infrastructures. Journal of Constructional Steel Research 2018; 149: 130-140.
[4] Xie J, Yan JB. Experimental studies and analysis on compressive strength of normal weight concrete at low temperatures. Structural Concrete 2018; 19(4): 1235-1244.
[5] Yan JB, Liew JYR, Zhang MH. Mechanical properties of mild steel and high strength steel S690 under low temperature relevant to Arctic environment. Materials & Design 2014; 61: 150-159.
[6] Xie J, Zhao X, Yan JB. Mechanical properties of high strength steel strand at low temperatures: Tests and analysis. Construction and Building Materials 2018; 189: 1076-1092.
[7] Yan JB, Xie J. Shear behaviour of headed stud connectors at low temperatures relevant to the Arctic environment. ASCE, Journal of Structural Engineering 2018; 144(9): 04018139.
[8] Virdi KS, Dowling PJ. Bond strength in concrete filled circular steel tubes.

Composite columns. CESLIC Report. CC11. London: Engineering Structures Laboratories, Civil Engineering Department, Imperial College, London; 1975.
[9] Morishita Y, Tomii M, Yoshimura K. Experimental studies on bond strength in concrete filled circular steel tubular columns subjected to axial loads. Transactions of Japan Concrete Institute; 1979. p. 351-8.
[10] Tomii M, Yoshimura K, Morishita Y. A method of improving bond strength in between steel tube and concrete core cast in circular steel tubular columns. Transactions of Japan Concrete Institute, 2; 1980. p. 319-26.
[11] Shakir-Khalil H, Pushout strength of concrete-filled steel hollow sections. Structural Engineer 1993; 71 (13): 230–243.
[12] Roeder CW, Cameron B, Brown CB, Composite action in concrete filled tubes, Journal of Structural Engineering. ASCE 1999; 125 (5): 477–484.
[13] Hunaiti YM. Bond strength in battened composite columns. Journal of Structural Engineering 1991; 117(3): 699–714.
[14] Hunaiti YM. Aging effect on bond strength in composite section. Journal of Materials in Civil Engineering 1994; 6(4): 469-473
[15] Petrus C, Hamid HA, Ibrahim A, Nyuin JD. Bond strength in concrete filled built-up steel tube columns with tab stiffeners. Canadian Journal of Civil Engineering 2011; 38: 627–637.
[16] Shakir-Khalil H. Resistance of concrete-filled steel tubes to push out forces. The Structural Engineer 1993; 71(13), 234–243.
[17] Shakir-Khalil H, Hassan NKA. Push-Out Resistance of concrete-Filled Tubes. Proceedings of the Sixth International Symposium on Tubular Structures, Melbourne, Australia, 14-16 December 1994; 285-291.
[18] Kilpatrick AE, Rangan BV. Influence of Interfacial Shear Transfer on Behavior of Concrete-Filled Steel Tubular Columns. ACI Structures Journal 1999; 96(4), 642-648.
[19] Tao Z, Song TY, Uy B, & Han LH. Bond behavior in concrete-filled steel tubes. Journal of Constructional Steel Research 2016; 120: 81-93.
[20] Aly T, Elchalakani M, Thayalan P, Patnaikuni I. Incremental collapse threshold for pushout resistance of circular concrete filled steel tubular columns. Journal of Constructional Steel Research 2010; 66: 11-18.
[21] Qu X, Liu Q. Bond strength between steel and self-compacting lower expansion concrete in composite columns. Journal of Constructional Steel Research 2017; 139: 176–187.
[22] Tao Z, Han LH, Uy B, Xian Chen X. Post-fire bond between the steel tube and concrete in concrete-filled steel tubular columns. Journal of Constructional Steel Research 2011; 67: 484–496.
[23] Wang WH, Han LH, Tan QH, Tao Z. Tests on the Steel–Concrete Bond Strength in Steel Reinforced Concrete (SRC) Columns After Fire Exposure. Fire Technology 2017; 53: 917–945.
[24] Song T; Tao Z, Han LH, Uy B. Bond behaviour of concrete-filled steel tubes at elevated temperatures. Journal of Structural Engineering 2017; 143(11): 04017147.

[25] GB51081-2015. (2015). Technical code for application of concrete under cryogenic circumstance. China Association for Engineering Construction Standardization, Chemical branch; Beijing, China.
[26] Xie J, Yan JB. Tests and analysis on thermal expansion behaviour of steel strand used in prestressed concrete structure under low temperatures. International Journal of Concrete Structures and Materials 2018; 12(1): 5.
[27] Cryogenic Division, LNG Materials and Fluids. 1977, National Bureau of Standards: Boulder, CO.
[28] Krstulovic-Opara N . Liquefied natural gas storage: Material behavior of concrete at cryogenic temperatures. Aci Materials Journal 2007; 104(3): 297-306.
[29] Kogbara RB, Iyengar SR, Grasley ZC. A review of concrete properties at cryogenic temperatures: Towards direct LNG containment. Construction and Building Materials 2013; 47: 760-770.
[30] Miura T. The properties of concrete at very low temperatures. Materials & Structures 1989; 22: 243-254.
[31] Liu X, Zhang MH, Chia KS, Yan J, Liew JYR. Mechanical properties of ultra-lightweight cement composite at low temperatures of 0 to -60ºC. Cement and Concrete Composites 2016; 73: 289-298.
[32] Chang X，Huang CK，Jiang DC． Push-out test of pre-stressing concrete filled circular steel tube columns by means of expansive cement. Construction and building materials 2009; 23( 1) : 491-497．
[33] Xie J, Yan JB. Tests and analysis on thermal expansion behaviour of steel strand used in prestressed concrete structure under low temperatures. International Journal of Concrete Structures and Materials 2018; 12(1): 91-100.
[34] Xue LH, Cai SH. Bond strength at interface of CFST columns, Part II. Building Science 1996; 4: 19-23. (In Chinese).
[35] BS EN 1994-1-1: 2004, Design of Composite Steel and Concrete Structures, Part1.1, General Rules and Rules for Building, British Standards Institution, London, 2004.
[36] ANSI/AISC 360-10, Specification for Structural Steel Buildings, American Institute of Steel Construction, Chicago (IL, USA), 2010.
[37] Cai SH. Modern concrete filled steel tube structure. Beijing: People's Communications Press，2003: 1-8. ( in Chinese) ).

Table 1 Mix proportions of different grades of normal weight concrete

| Mix | Cement ($kg/m^3$) | Mineral ($kg/m^3$) | Fly ash ($kg/m^3$) | Coarse sand ($kg/m^3$) | Fine sand ($kg/m^3$) | Gravel ($kg/m^3$) | Water ($kg/m^3$) | SP ($kg/m^3$) | w/c |
|---|---|---|---|---|---|---|---|---|---|
| C30 | 220 | 81 | 74 | 719 | 176 | 940 | 165 | 8.2 | 0.75 |
| C45 | 300 | 105 | 66 | 619 | 155 | 1005 | 165 | 10.4 | 0.55 |
| C60 | 410 | 110 | 65 | 540 | 135 | 1018 | 160 | 12.9 | 0.39 |

Table 2 Details and results of push-out tests on CFST columns

| Item | $D$ (mm) | $t$ (mm) | $L$ (mm) | $D/t$ | $L/D$ | $T$ (ºC) | $f_{cu,T}$ (MPa) | $f_{cu,a}$ (MPa) | $\tau_{u,t}$ MPa | $\tau_{u,p}$ MPa | $\tau_{u,t}$ / $\tau_{u,p}$ |
|---|---|---|---|---|---|---|---|---|---|---|---|
| | (1) | (2) | (3) | (1)/(2) | (3)/(1) | (6) | (7) | (8) | (9) | (10) | (9)/(10) |
| C1 | 133 | 4.50 | 360 | 29.6 | 2.71 | -60 | 53.5 | 43.9 | 2.15 | 1.90 | 1.13 |
| C2 | 133 | 4.50 | 360 | 29.6 | 2.71 | 30 | 43.9 | 43.9 | 0.62 | 0.60 | 1.02 |
| C3 | 133 | 4.50 | 360 | 29.6 | 2.71 | -30 | 45.3 | 43.9 | 1.79 | 1.47 | 1.22 |
| C4 | 133 | 4.50 | 360 | 29.6 | 2.71 | -80 | 65.8 | 43.9 | 2.39 | 2.19 | 1.09 |
| C5 | 133 | 4.50 | 360 | 29.6 | 2.71 | -60 | 47.2 | 35.0 | 3.51 | 1.90 | 1.85 |
| C6 | 133 | 4.50 | 360 | 29.6 | 2.71 | -60 | 65.5 | 55.0 | 1.31 | 1.90 | 0.69 |
| C7 | 133 | 3.00 | 360 | 44.3 | 2.71 | -60 | 53.5 | 43.9 | 2.15 | 1.90 | 1.13 |
| C8 | 133 | 5.75 | 360 | 23.1 | 2.71 | -60 | 53.5 | 43.9 | 2.70 | 1.90 | 1.42 |
| C9 | 133 | 4.50 | 210 | 29.6 | 1.58 | -60 | 53.5 | 43.9 | 2.12 | 1.90 | 1.12 |
| C10 | 133 | 4.50 | 560 | 29.6 | 4.21 | -60 | 53.5 | 43.9 | 2.28 | 1.90 | 1.20 |
| S1 | 120 | 4.00 | 360 | 30.0 | 3.00 | -60 | 53.5 | 43.9 | 1.55 | 1.04 | 1.50 |
| S2 | 120 | 4.00 | 360 | 30.0 | 3.00 | 30 | 43.9 | 43.9 | 0.58 | 0.33 | 1.78 |
| S3 | 120 | 4.00 | 360 | 30.0 | 3.00 | -30 | 45.3 | 43.9 | 0.90 | 0.80 | 1.13 |
| S4 | 120 | 4.00 | 360 | 30.0 | 3.00 | -80 | 60.7 | 43.9 | 1.83 | 1.19 | 1.53 |
| S5 | 120 | 4.00 | 360 | 30.0 | 3.00 | -60 | 47.2 | 35.0 | 2.22 | 1.04 | 2.14 |
| S6 | 120 | 4.00 | 360 | 30.0 | 3.00 | -60 | 65.5 | 55.0 | 1.29 | 1.04 | 1.25 |
| S7 | 120 | 2.75 | 360 | 43.6 | 3.00 | -60 | 53.5 | 43.9 | 1.01 | 1.04 | 0.97 |
| S8 | 120 | 5.00 | 360 | 24.0 | 3.00 | -60 | 53.5 | 43.9 | 1.45 | 1.04 | 1.40 |
| S9 | 120 | 4.00 | 210 | 30.0 | 1.75 | -60 | 53.5 | 43.9 | 2.03 | 1.04 | 1.96 |
| S10 | 120 | 4.00 | 510 | 30.0 | 4.25 | -60 | 53.5 | 43.9 | 1.77 | 1.04 | 1.71 |
| Mean | | | | | | | | | | | 1.36 |
| Cov | | | | | | | | | | | 0.27 |

$f_{cu,T}$ denotes compressive strength of concrete at low temperatures; $f_{cu,a}$ denotes compressive strength of concrete at ambient temperatures; $\tau_{u,t}$ denotes experimental ultimate bond strength; $\tau_{u,p}$ denotes ultimate bond strength predicted by Eqn. (2).

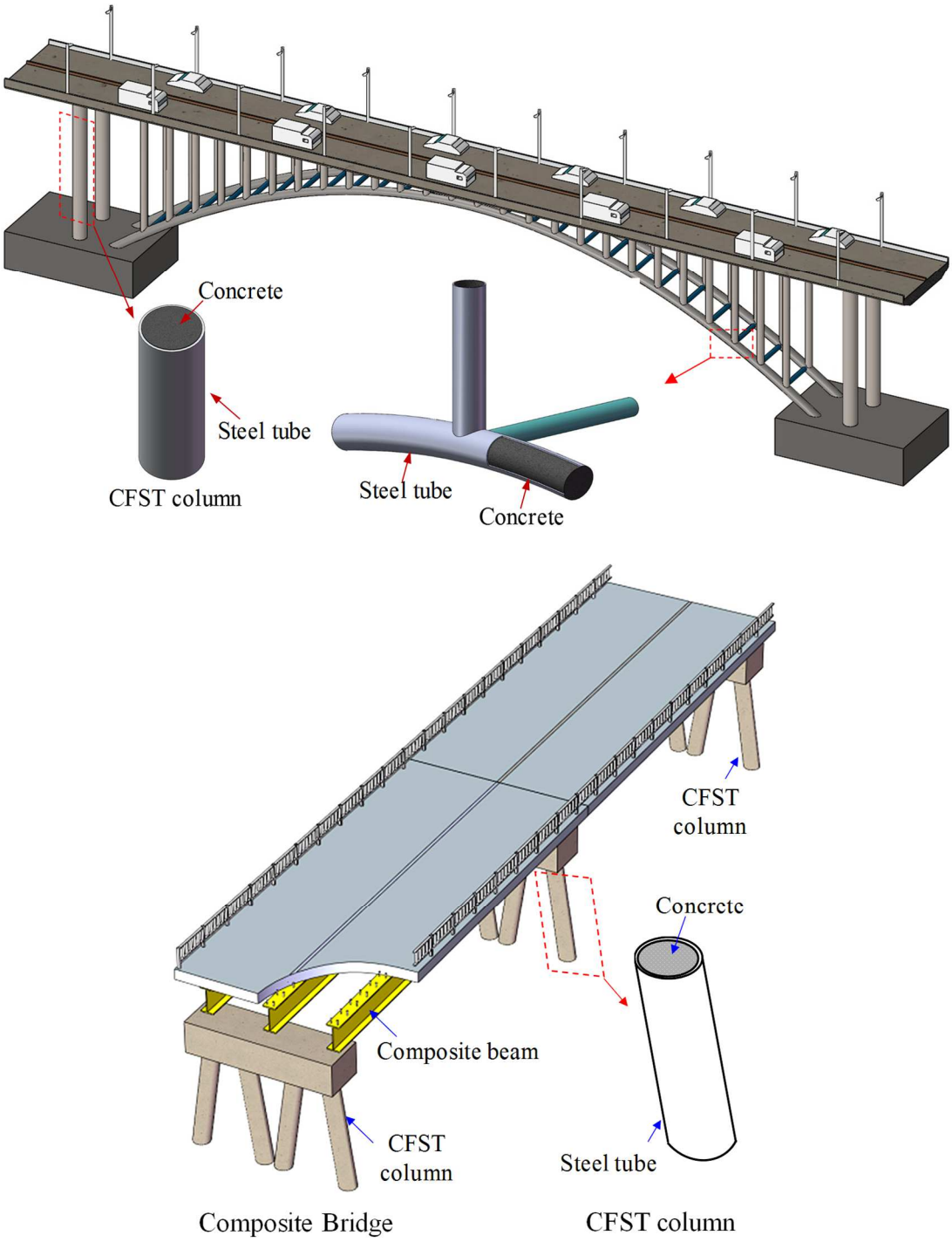


Fig. 1 CFST columns in steel-concrete composite bridges

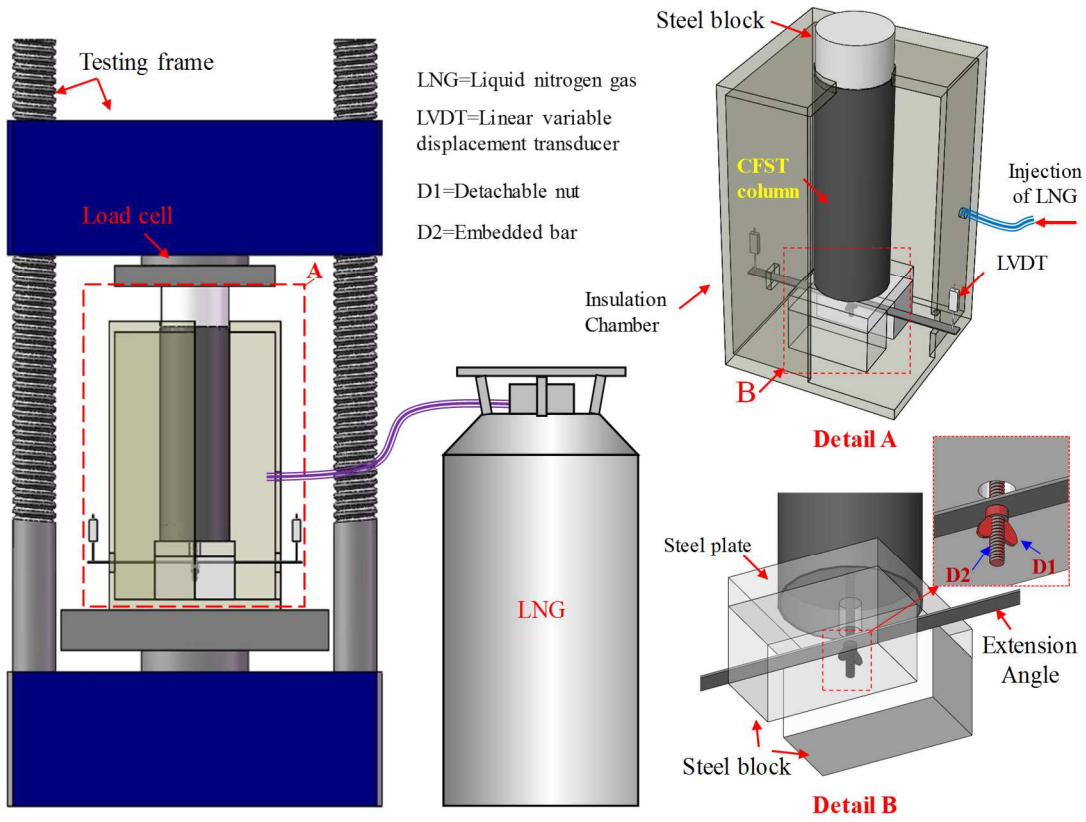


(a) Test setup

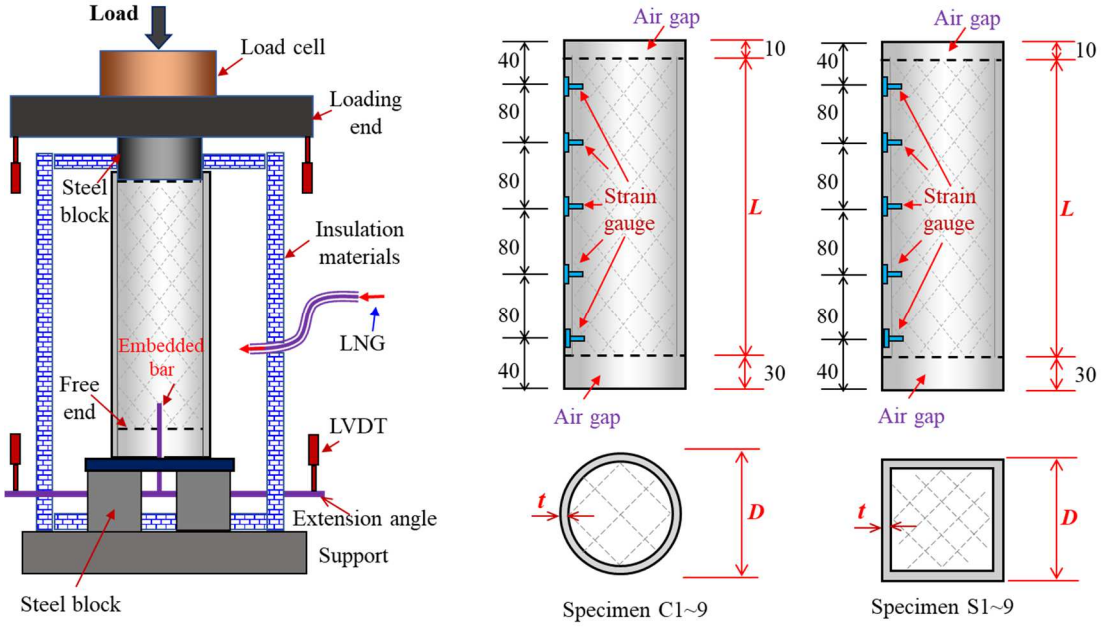


(b) Loading and measurements

Fig. 2 Push-out test setup

(a) Steel tubes prepared for casting

(b) CFST columns after casting

(c) CFST columns for the push-out tests

Fig. 3 Preparation of CFST columns for the push-out tests

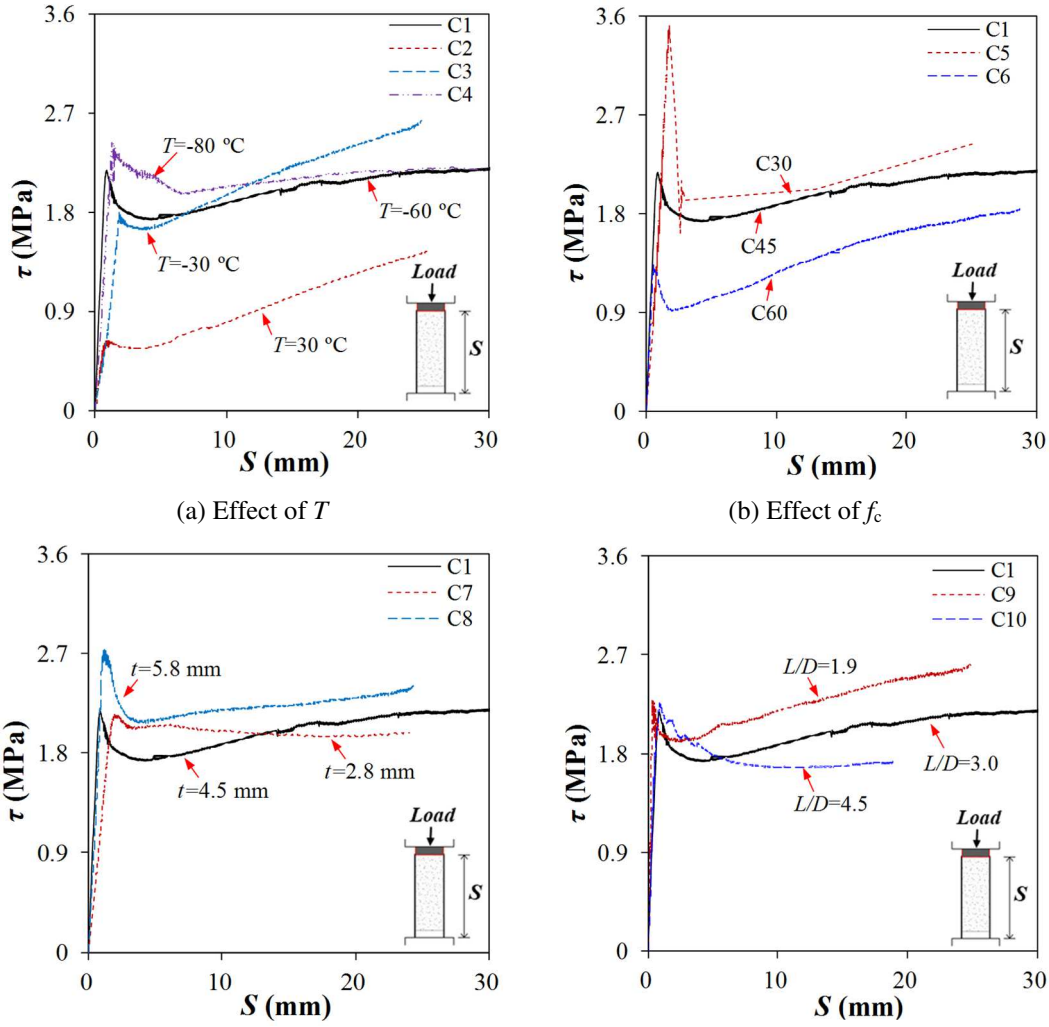


(a) Effect of $T$ (b) Effect of $f_c$

(c) Effect of $t$ (d) Effect of $L/D$

Fig. 4 Bond stress versus slip curves of circular CFST columns

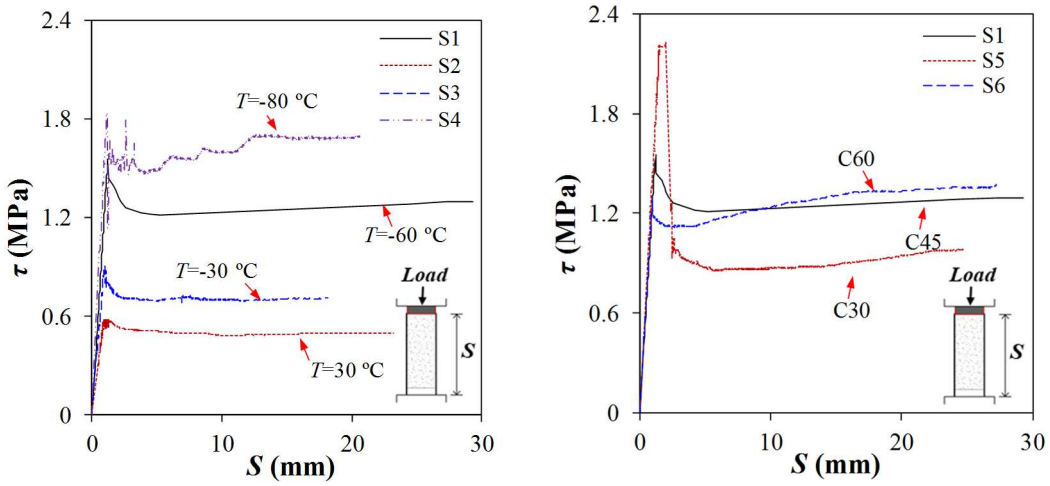


(a) Effect of $T$ (b) Effect of $f_c$

(c) Effect of $t$ (d) Effect of $L/B$

Fig. 5 Bond stress versus slip curves of square CFST columns

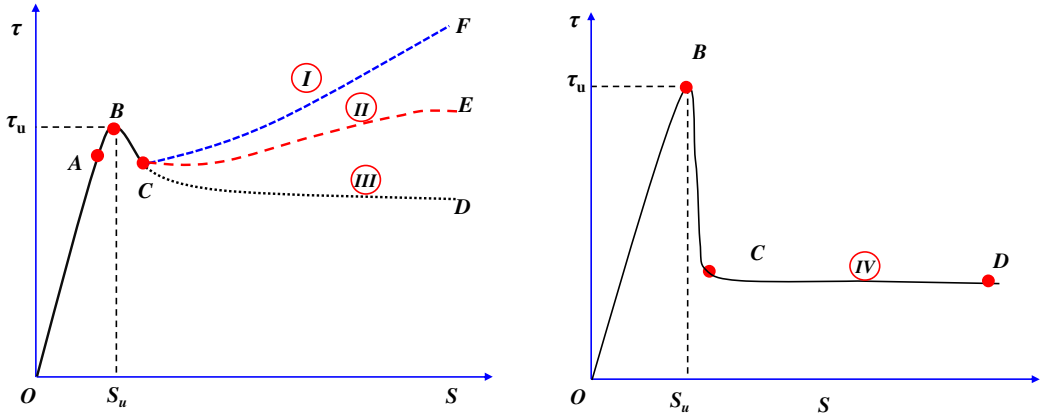


(a) Type I~III (b) Type IV

Fig. 6 Generalized bond stress versus slip curves of CFST at low temperatures

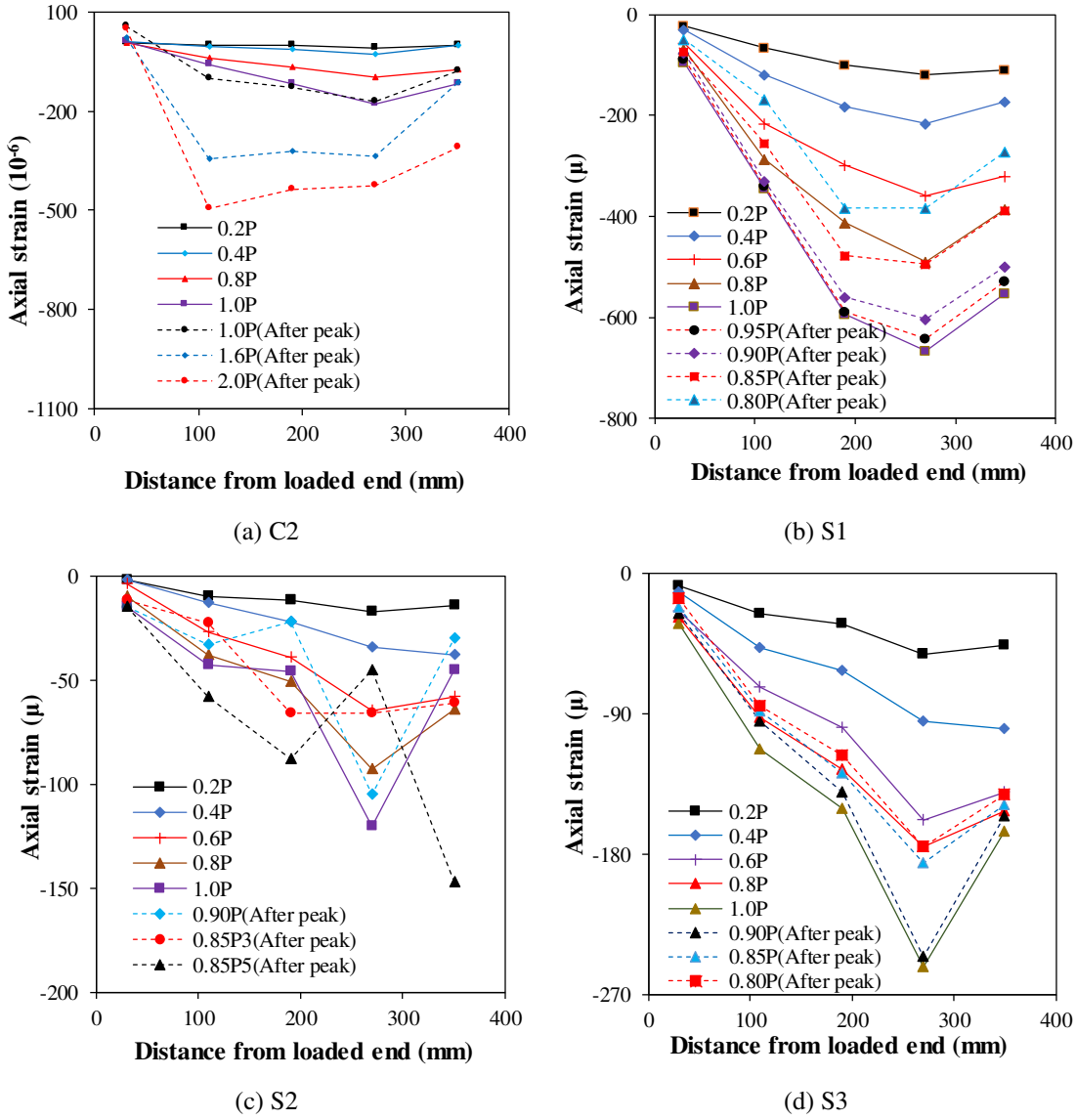


(a) C2

(b) S1

(c) S2

(d) S3

Fig. 7 Distribution of strain along height of the external steel tube in CFST column

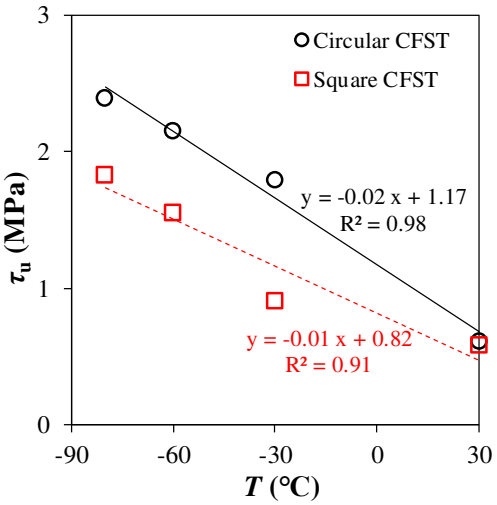


(a) Effect of temperature

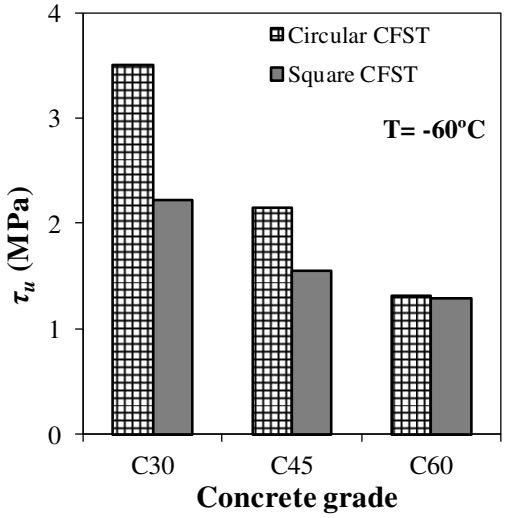


(b) Effect of different grades of concrete

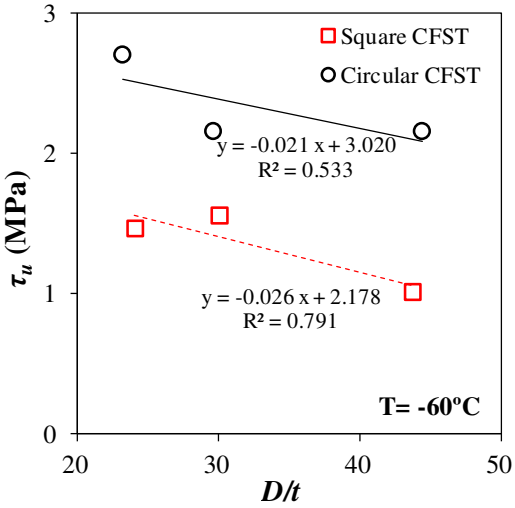


(c) Effect of thickness of steel tube

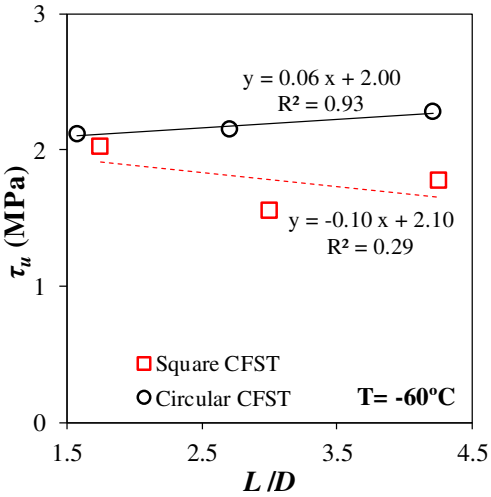


(d) Effect of *L/D* or *L/B* ratio

Fig. 8 Effect of different parameters on bond stress of CFST column at low temperatures

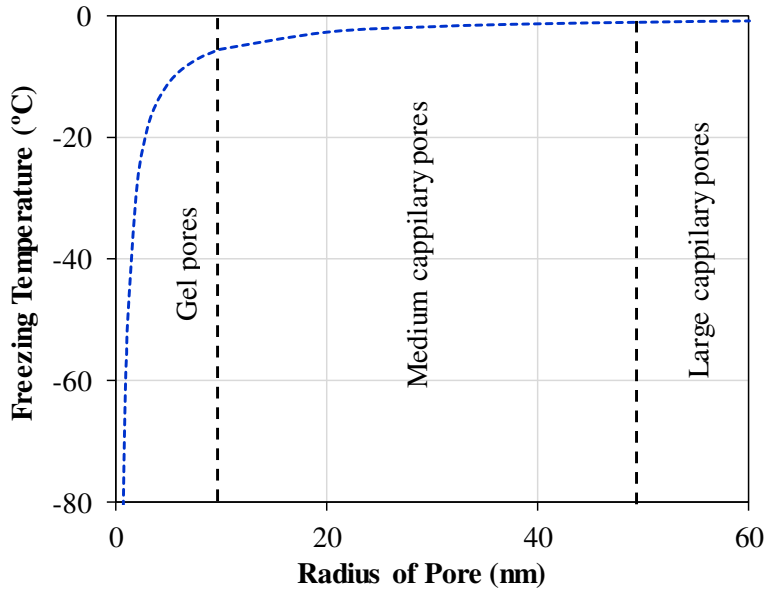


Fig. 9 Freezing temperature versus radius of pore relationship

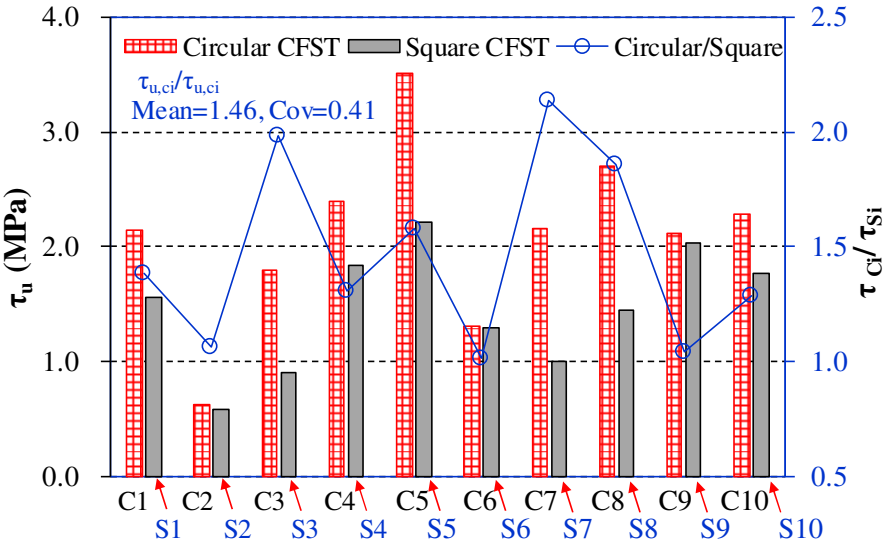


Fig. 10 Comparisons of ultimate bond strength between circular and square CFST columns

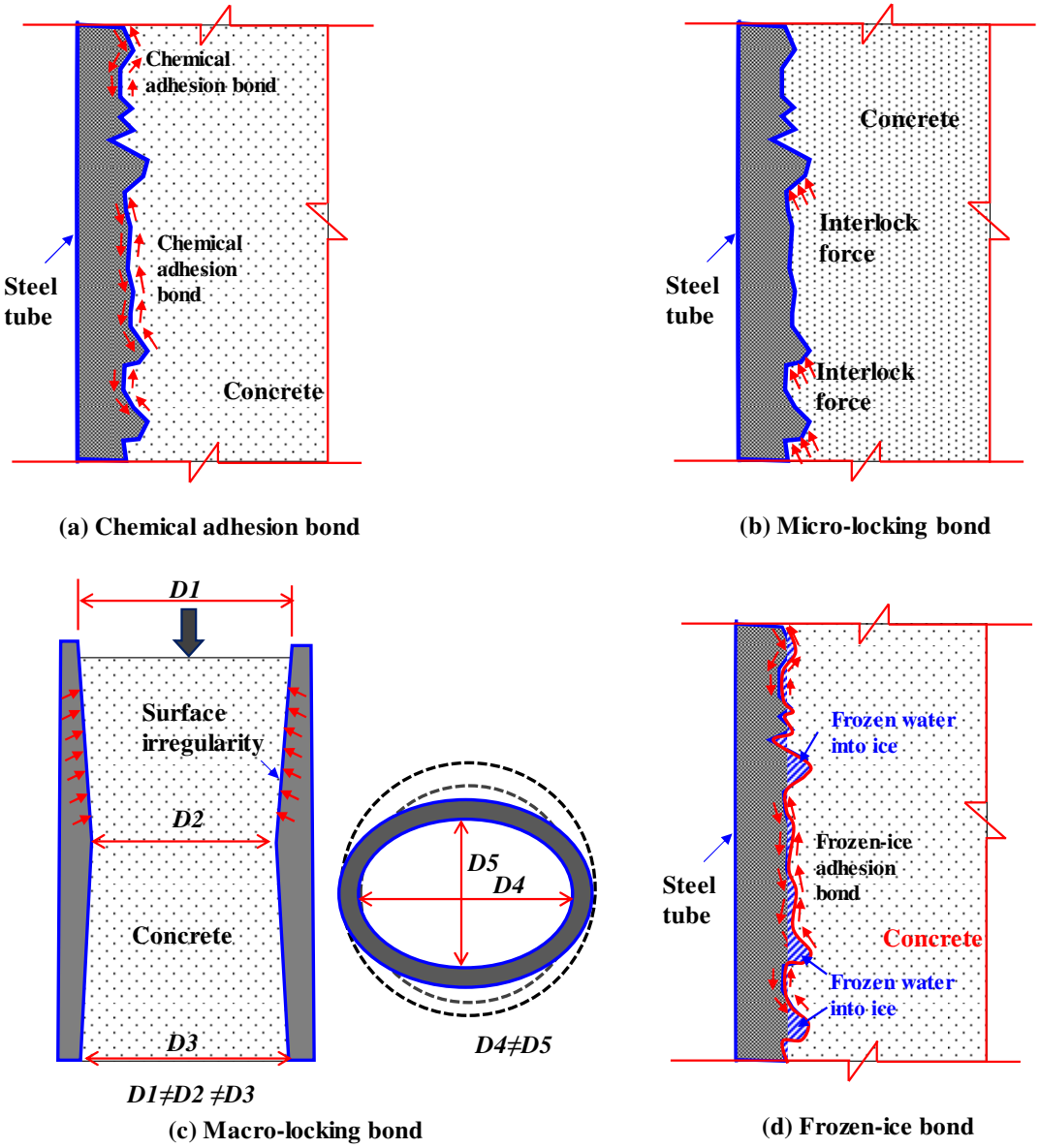


Fig. 11 Illustration on different components of bond stress in CFST column at low temperatures

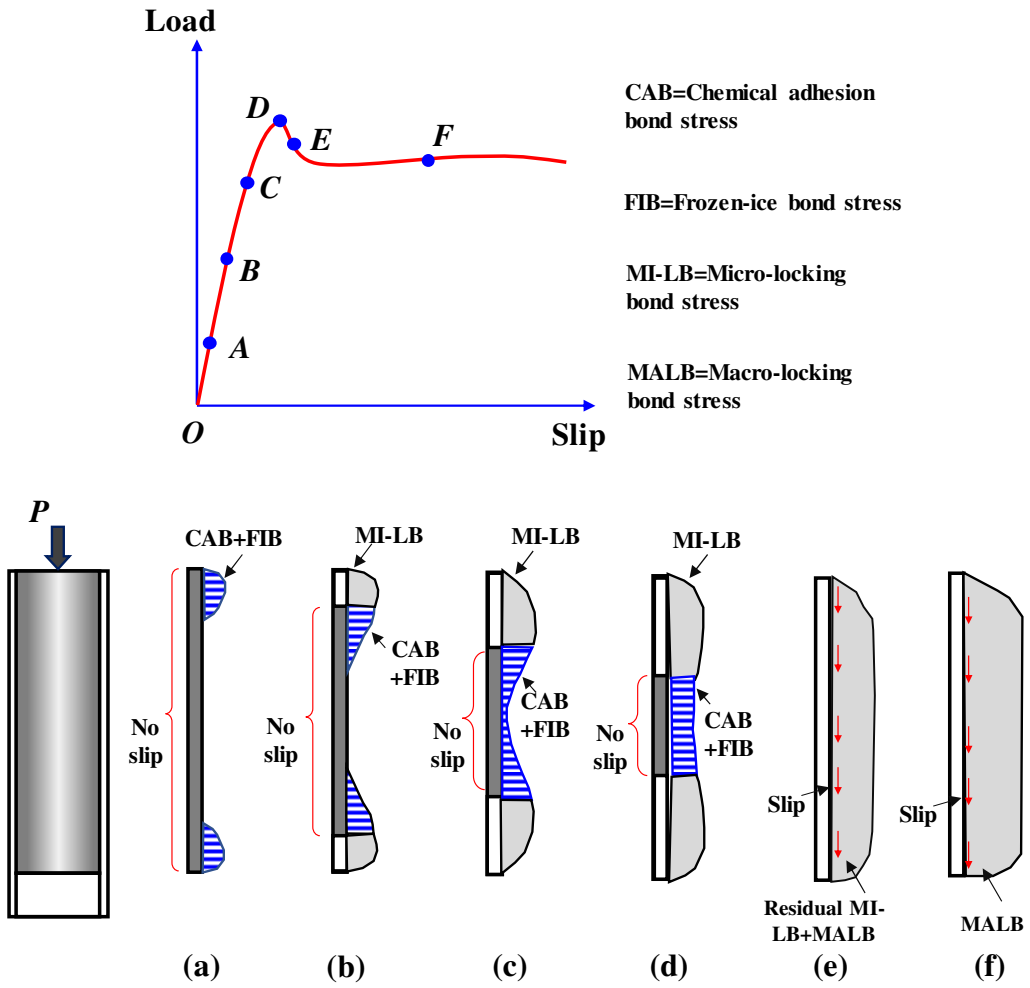


Fig. 12 General illustration on mechanisms on developments of bond stress versus slip behaviour

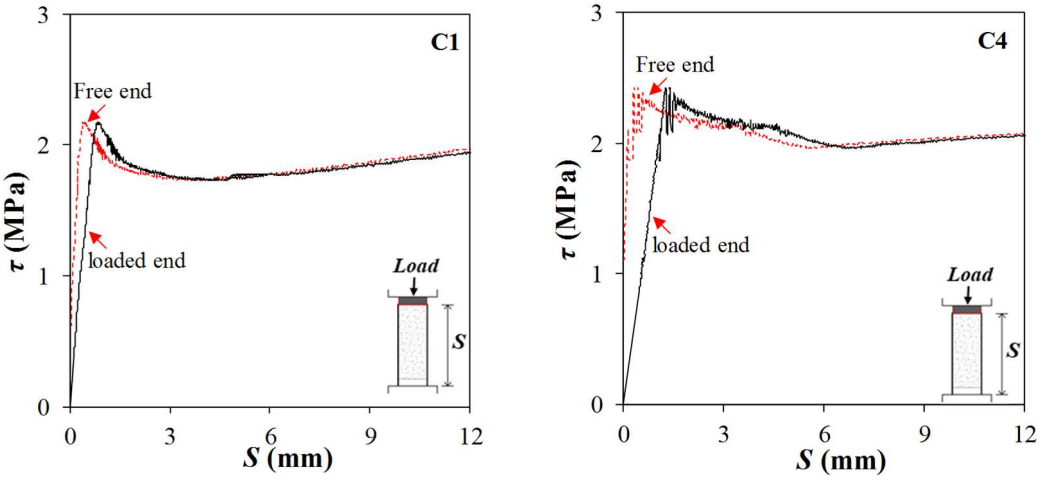


(a) C1 (b) C4

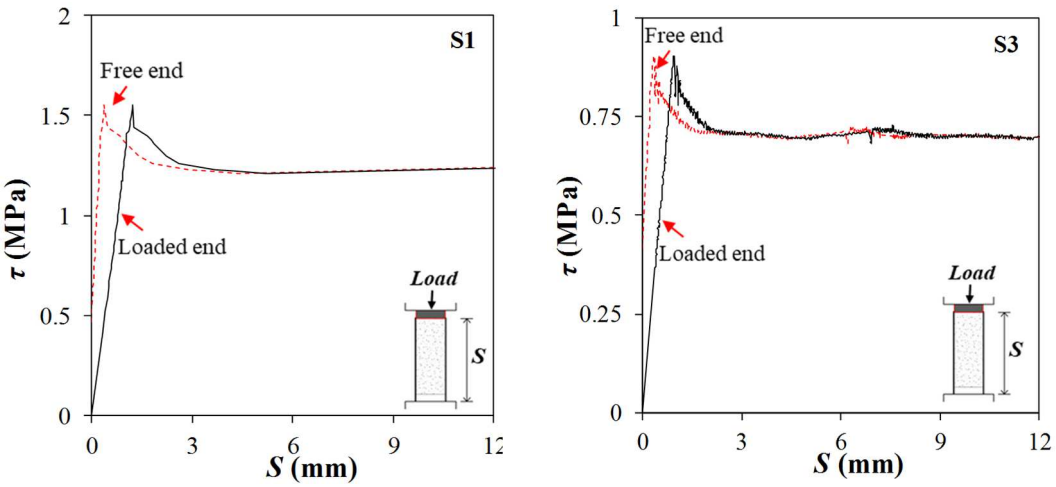


(c) S1 (d) S3

Fig. 13 Comparisons of bond stress versus slip curves recorded at loaded and free ends of CFST columns

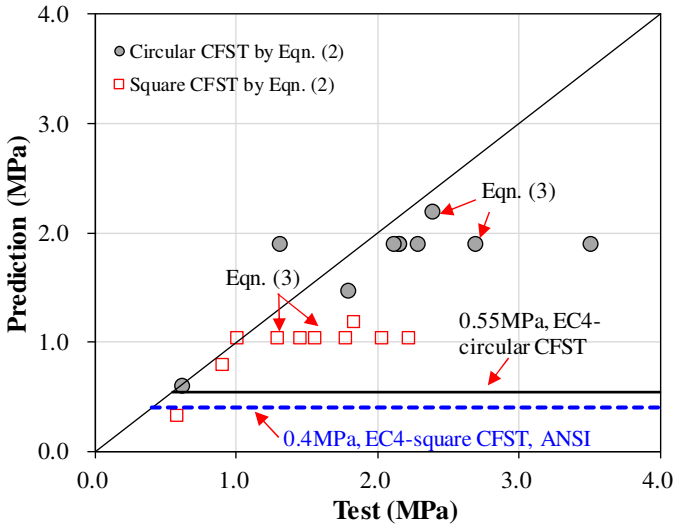


Fig. 14 Comparisons of predictions with test results